

# Quadratic NLS Simulations

Realeboga Dikole

January 19, 2021

## 1 Numerical Solution of the Quadratic NLS

The equation in question is the quadratic nonlinear Schrödinger equation and it states

$$(i + \lambda) \frac{\partial \psi}{\partial t} - \frac{\partial^2 \psi}{\partial x^2} - 6\psi^2 = -4\psi + b(\psi - \psi^*), \quad (1)$$

where  $\lambda = 0$  in the simulations below. The numerical method used here is the Fourier spectral differentiation method, where we take  $\mathcal{D}_N^{(2)}$  as an approximation of spatial derivatives, with the superscript of 2 denoting the order of the derivative and subscript denotes that the matrix is  $N \times N$ . The time derivatives are approximated using the centered differences as follows

$$\frac{\partial \psi(x, t)}{\partial t} \approx \frac{\psi_j^{n+1} - \psi_j^{n-1}}{2\tau} + \mathcal{O}(\tau^2), \quad (2)$$

where we have defined  $\psi(x, t)$  in its discrete form as  $\psi(x_j, t_n) = \psi_j^n$ . For approximating the spatial part of  $\psi(x, t)$  we make use of differentiation matrix  $\mathcal{D}_N^{(2)}$  which is given by the following

$$\mathcal{D}_N^{(2)} = \begin{pmatrix} \vdots & & & & & \\ \ddots & -\frac{1}{2} \csc^2\left(\frac{2h}{2}\right) & & & & \\ \ddots & \frac{1}{2} \csc^2\left(\frac{h}{2}\right) & & & & \\ \ddots & -\frac{\pi^2}{3h^2} - \frac{1}{6} & & & & \\ & \frac{1}{2} \csc^2\left(\frac{h}{2}\right) & & \ddots & & \\ & -\frac{1}{2} \csc^2\left(\frac{2h}{2}\right) & & \ddots & & \\ \vdots & & & & \ddots & \end{pmatrix}. \quad (3)$$

The matrix  $\mathcal{D}_N^{(2)}$  is an operator and it acts on  $\psi_j^2$  at each time step  $\tau$  to approximate the derivative at the particular time step. The discrete form of (1) reads

$$\psi_j^{n+1} = \psi_j^{n-1} + \left(\frac{2\tau}{i + \lambda}\right) \left\{ \frac{\pi^2}{L^2} \mathcal{D}_N^{(2)} \psi_j^n + 6(\psi_j^n)^2 - 4\psi_j^n + b(\psi_j^n - (\psi_j^n)^*) \right\}, \quad (4)$$

See the plots below for the simulations of (1) — a stationary solution known as the *fundamental soliton/ sech mode* is considered as an initial condition when  $b = 0$  and  $\lambda = 0$ . The *fundamental soliton* reads

$$u_s(x) = \text{sech}^2(x), \quad (5)$$

where the subscript  $s$  denotes the fact that this is a stationary solution. The simulation is done on the interval  $[-20\pi, 20\pi]$  and only the interval  $[-2\pi, 2\pi]$  is shown for better viewing. The time variable  $t$  runs on the interval  $[0, 50]$ .

(i) **Solution for  $b = 0, \lambda = 0$ :**

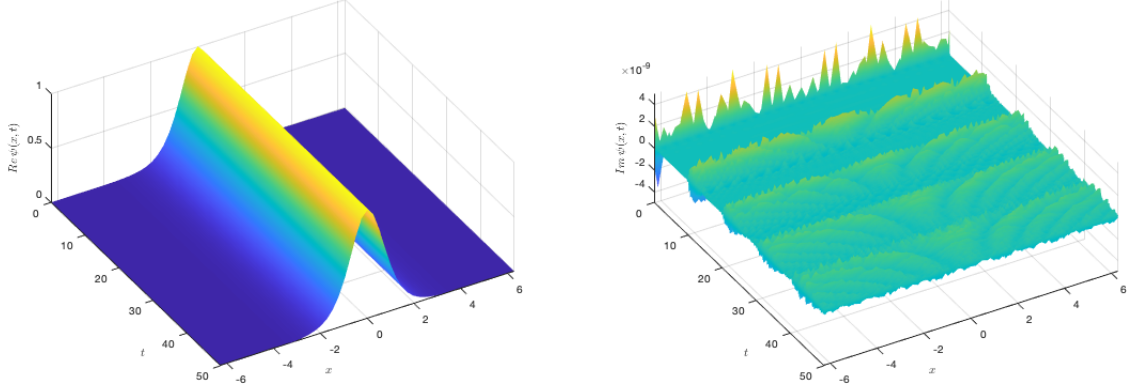


Figure 1.1 The Fourier spectral solution of the quadratic NLS. The real part solution is on the left, and the imaginary part of the solution if on the right.

## 2 Fundamental soliton and its instability

To investigate the stability of (5) we add a small perturbation and evolve it according to (1). The choice of our perturbation is  $\epsilon \cos(x)$ , where  $\epsilon$  is small enough to ensure the solutions don't blow up completely. The new initial conditions now reads

$$u(x) = u_s(x) + \epsilon \cos(x) \quad (6)$$

### 2.1 Numerical results

All the simulations below were performed without the inclusion of the friction term  $\lambda \partial_t \psi$  in (??). See the plots below.

(i) **Solution for  $b = -3, \lambda = 0$  and  $\epsilon = 10^{-13}$ :**

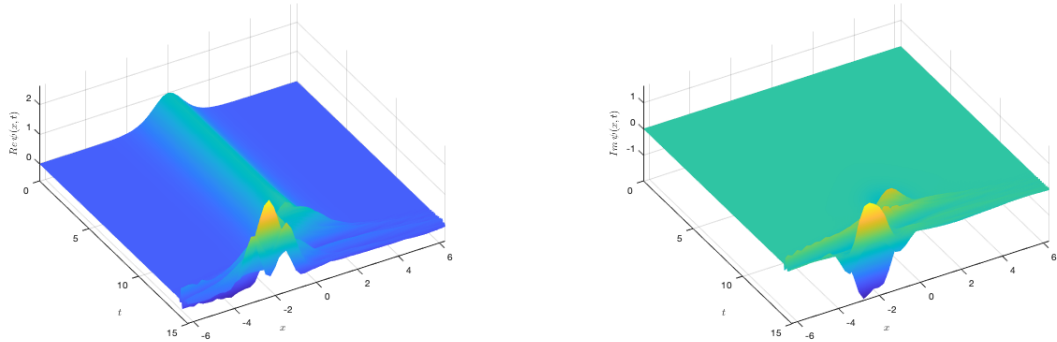


Figure 2.1.1 (a) The real (left) and imaginary (right) parts of  $\psi(x, t)$

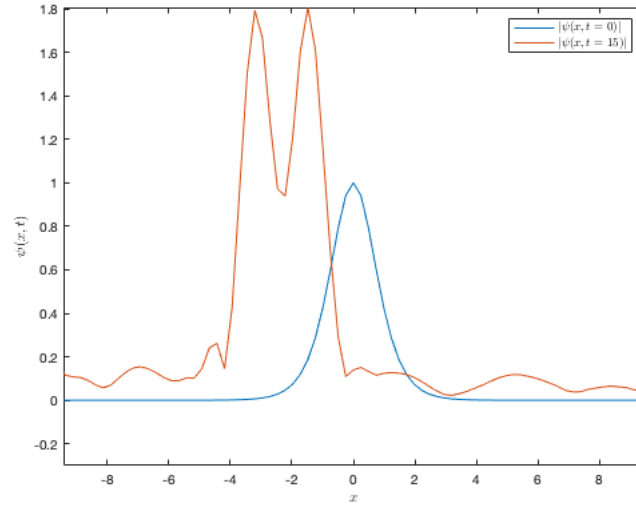


Figure 2.1.1 (b) The graph of  $|\psi(x, t)|$  at showing the initial condition (blue) at time  $t = 0$  and the disintegration of the initial wave form at time  $t = 15$ .

(ii) **Solution for  $b = -2$ ,  $\lambda = 0$  and  $\epsilon = 10^{-3}$ :**

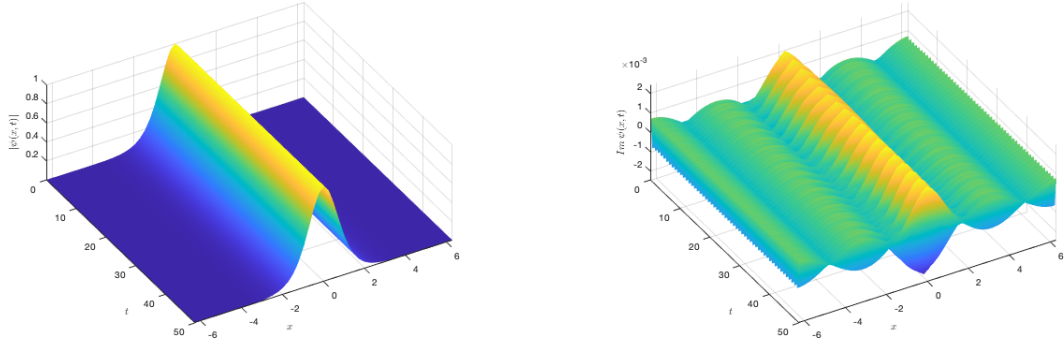


Figure 2.1.2 The real (left) and imaginary (right) parts of  $\psi(x, t)$

(iii) **Solution for  $b = -1$ ,  $\lambda = 0$  and  $\epsilon = 10^{-3}$ :**

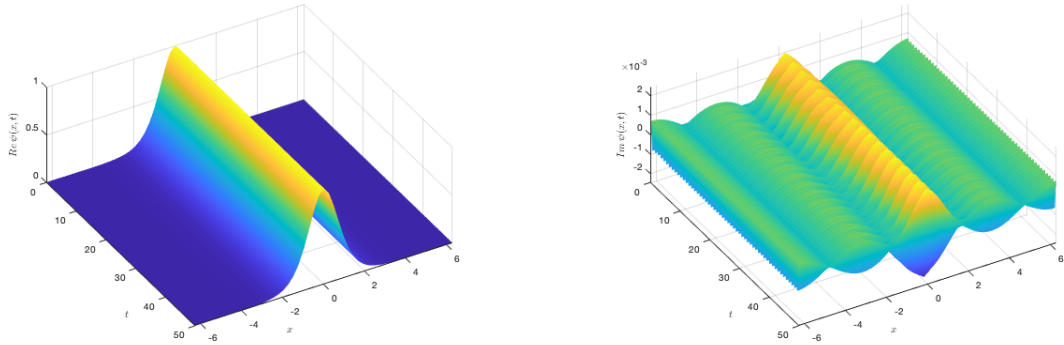


Figure 2.1.3 The real (left) and imaginary (right) parts of  $\psi(x, t)$

(iv) **Solution for  $b = 0$ ,  $\lambda = 0$  and  $\epsilon = 10^{-3}$ :**

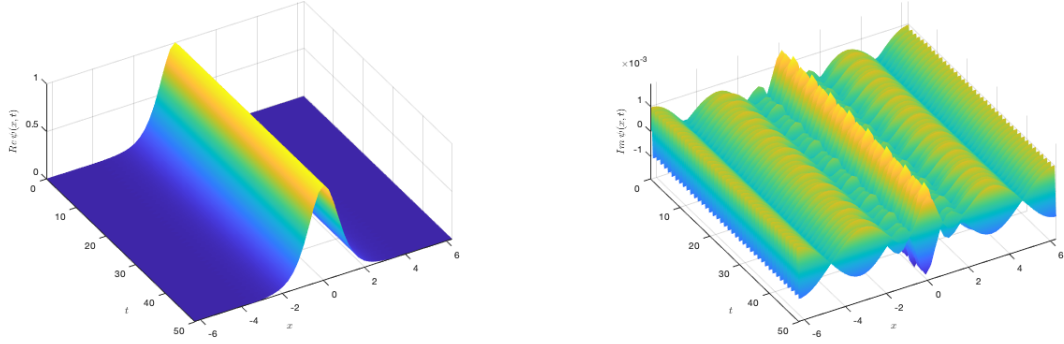


Figure 2.1.4 The real (left) and imaginary (right) parts of  $\psi(x, t)$

(v) **Solution for  $b = 1$ ,  $\lambda = 0$  and  $\epsilon = 10^{-3}$ :**

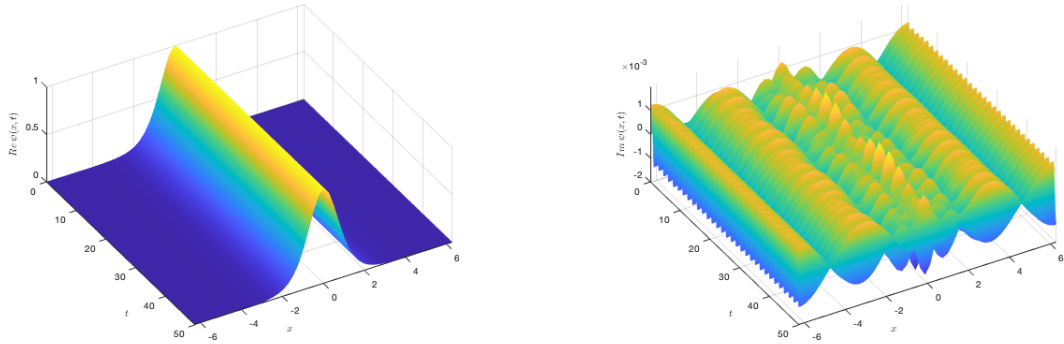


Figure 2.1.5 The real (left) and imaginary (right) parts of  $\psi(x, t)$

(vi) **Solution for  $b = 2$ ,  $\lambda = 0$  and  $\epsilon = 10^{-13}$ :**

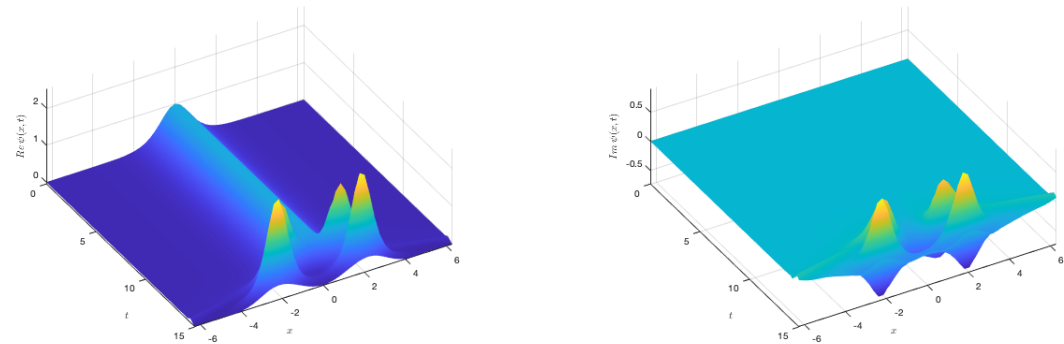


Figure 2.1.6 (a) The real (left) and imaginary (right) parts of  $\psi(x, t)$

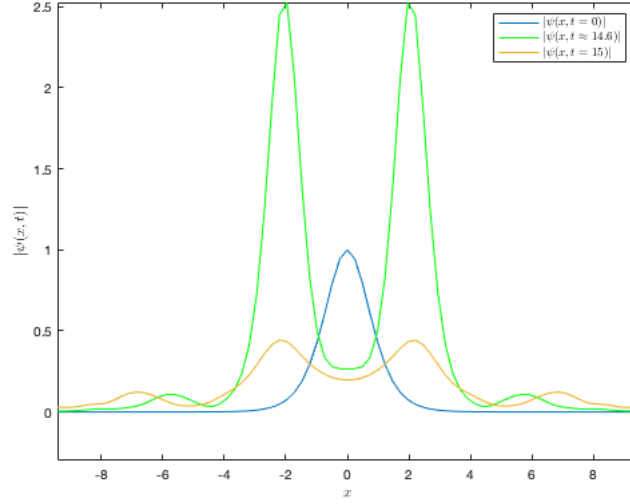


Figure 2.1.6 (b) The graph of  $|\psi(x, t)|$  at showing the initial condition (blue) at time  $t = 0$  and the disintegration of the initial wave form (green) at time  $t \approx 14.6$ , where the soliton jumps to maximum  $|\psi| = 2.5$  and then drops lower (orange) than  $|\psi| = 0.5$  at  $t = 15$ .

### 3 Inclusion of the damping coefficient

We have previously shown the numerical simulations of (1) and its instability in the absence of the friction term. Now we consider the same perturbed initial condition (6) for the nonzero friction coefficient  $\lambda$ . See plots below.

(i) **Solution for  $b = -3$ ,  $\lambda = 0.3$  and  $\epsilon = 10^{-5}$ :**

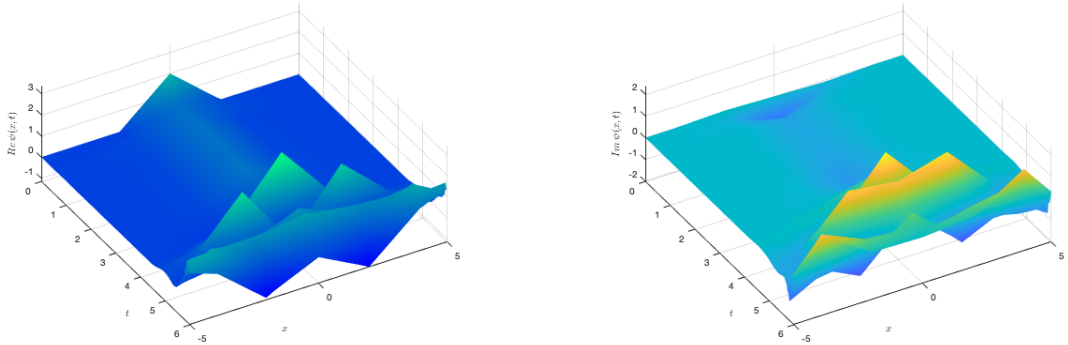


Figure 3.1 The real (left) and imaginary (right) parts of  $\psi(x, t)$

(ii) **Solution for  $b = -2$ ,  $\lambda = 0.3$  and  $\epsilon = 10^{-5}$ :**

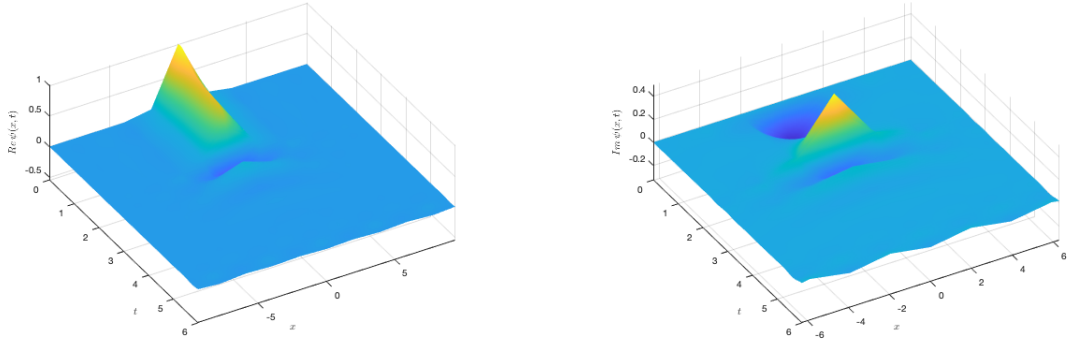


Figure 3.2 The real (left) and imaginary (right) parts of  $\psi(x, t)$

(iii) **Solution for  $b = -1$ ,  $\lambda = 0.3$  and  $\epsilon = 10^{-5}$ :**

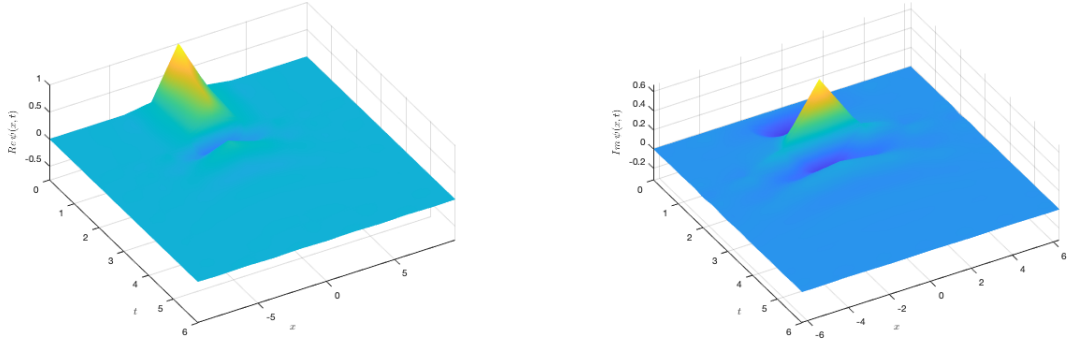


Figure 3.3 The real (left) and imaginary (right) parts of  $\psi(x, t)$

(iv) **Solution for  $b = 0$ ,  $\lambda = 0.3$  and  $\epsilon = 10^{-5}$ :**

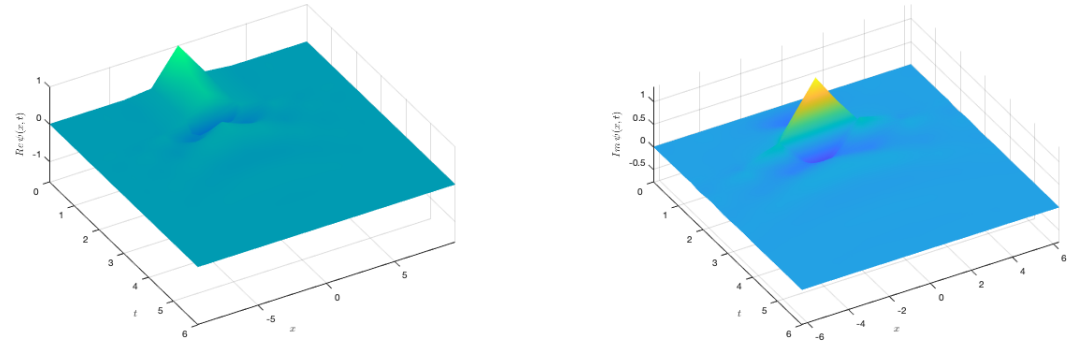


Figure 3.4 The real (left) and imaginary (right) parts of  $\psi(x, t)$

(v) **Solution for  $b = 1$ ,  $\lambda = 0.3$  and  $\epsilon = 10^{-5}$ :**

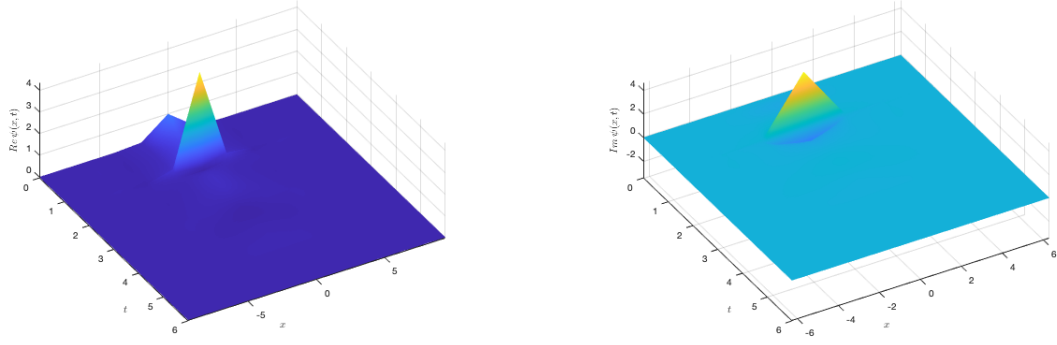


Figure 3.5 The real (left) and imaginary (right) parts of  $\psi(x, t)$

(vi) **Solution for  $b = 2$ ,  $\lambda = 0.3$  and  $\epsilon = 10^{-5}$ :**

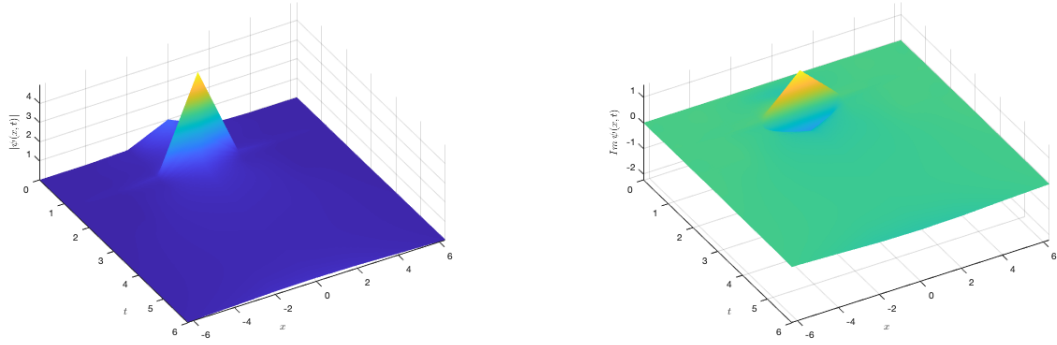


Figure 3.6 The real (left) and imaginary (right) parts of  $\psi(x, t)$

## 4 Twisted modes of the QNLS

In this section we consider the *sech-tanh* initial condition and propagate it according to (1) — the equation (1) possesses two sets of solution known as the *twisted* or *sech-tanh* mode; the solutions are given as

$$u_T(x) = 2 \operatorname{sech}^2(2x) \pm 2i \operatorname{sech}(2x) \tanh(2x). \quad (7)$$

We simulate the two sets of solutions below.

(a) **Case 1**

Here we consider the first *sech-mode*  $u_T(x) = 2 \operatorname{sech}^2(2x) + 2i \operatorname{sech}(2x) \tanh(2x)$  as the initial condition and plugging this into (4) yields the following results:

(i) **Solution for  $b = 0$  and  $\lambda = 0$ :**

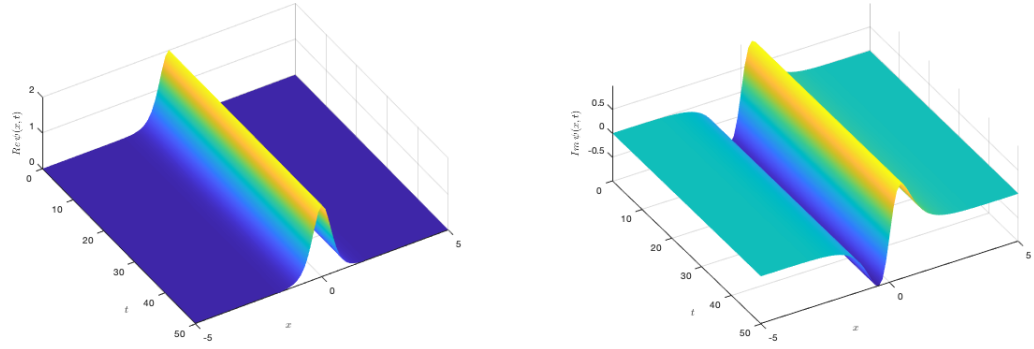


Figure 4.1 The real (left) and imaginary (right) parts of  $\psi(x, t)$

**Solution for  $b = 0$ ,  $\lambda = 0.1$ :**

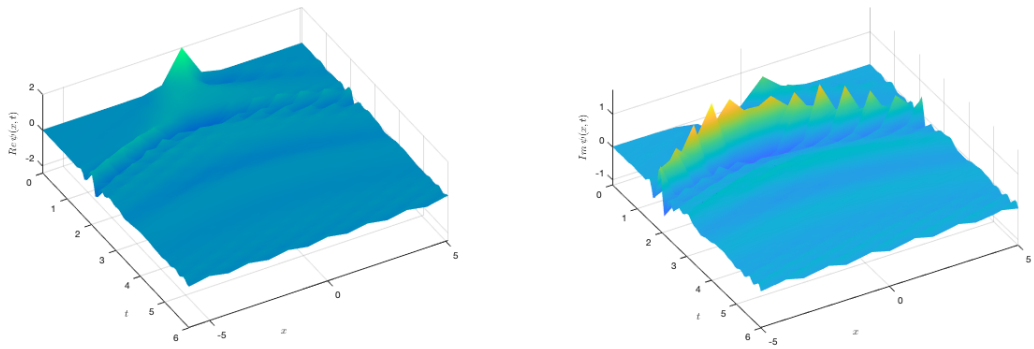


Figure 4.2 The real (left) and imaginary (right) parts of  $\psi(x, t)$



(b) **Case 2**

We now consider  $u_T(x) = 2 \operatorname{sech}^2(2x) - 2i \operatorname{sech}(2x) \tanh(2x)$  as the initial condition. Plugging into (4) yields the following results:

(i) **Solution for  $b = 0$  and  $\lambda = 0$ :**

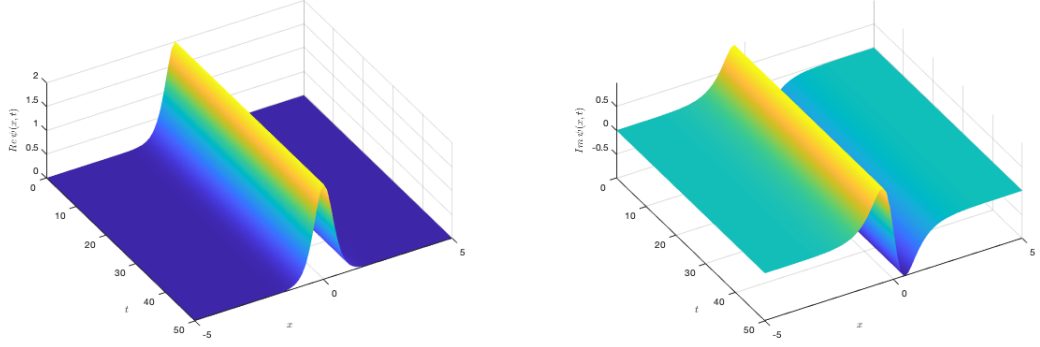


Figure 4.3 The real (left) and imaginary (right) parts of  $\psi(x, t)$

(ii) **Solution for  $b = 0$  and  $\lambda = 0.1$ :**

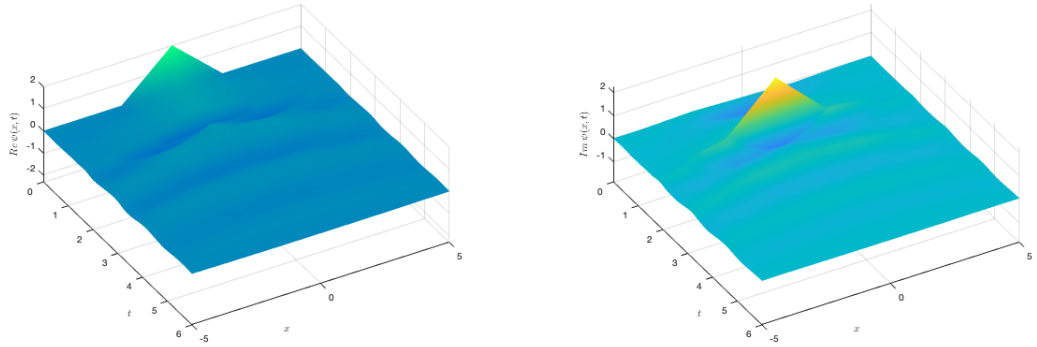


Figure 4.4 The real (left) and imaginary (right) parts of  $\psi(x, t)$